Front. Optoelectron. 2015, 8(3): 289–297
DOI 10.1007/s12200-015-0527-6

RESEARCH ARTICLE

Improvement of electrical and photovoltaic properties of methyl red dye based photoelectrochemical cells in presence of single walled carbon nanotubes

Sujata CHAKRABORTY, Nabin Baran MANIK (✉)

Condensed Matter Physics Research Center, Department of Physics, Jadavpur University, Kolkata 700032, India

Abstract In this work, we investigated the effect of single walled carbon nanotubes (SWCNT) on the electrical and photovoltaic properties of methyl red (MR) dye based photoelectrochemical cell (PEC). MR dye based PEC with $LiClO_4$ as ion salt were fabricated with and without mixing SWCNT. The cells were characterized through electrical and optical measurements. The performance of the devices changed drastically in presence of SWCNT. The transition voltage and trap energy of the cells were estimated from the steady-state dark current voltage (*I*-*V*) analysis. The transition voltage and trap energy decreased for MR dye cell in presence of SWCNT. Open circuit voltage (V_{oc}), short circuit current (J_{sc}), fill factor (*FF*) and power conversion efficiency (η) increased due to the addition of SWCNT. Further measurement of the transient photocurrent showed that the growth and decay of photocurrent was quite faster in presence of SWCNT. The photocurrent decay with time was fitted for both the cells and found to follow a power law relation which indicates dispersive transport mechanism with exponential trap states distributed in between lowest unoccupied molecular orbital (LUMO) and highest occupied molecular orbital (HOMO) levels. Possible interpretation is done on the lowering of trap energy with the photocurrent. These results suggest that SWCNT lowers the trap energy of the cells by providing efficient percolation pathways for the conduction of charges. It is expected that due to lowering of trap energy the residing time of the free carriers within the traps decreases. In other words, it may also be said that the charge recombination decreases. These factors affect the overall conduction of charges and improve the electrical and photovoltaic properties.

Keywords methyl red (MR), single walled carbon nanotubes (SWCNT), photoelectrochemical cell (PEC), trap energy, percolation pathways

1 Introduction

Recently organic dye based solid state photoelectrochmical cells (PECs) have emerged as an immensely attracting field mainly due to their low cost, light weight and high flexibility [1–4]. They are being widely used as photovoltaic devices to harvest solar energy. In any PEC, organic dye is mixed with a solid electrolyte. The ionic conductivity in these PECs plays a vital role to enhance the quantum efficiency of these devices. However, compared to their inorganic counterparts, these cells suffer from low efficiency and stability [5–8]. The important factor is the presence of traps in these organic systems, which severely affect their performance [9–11]. Due to the presence of traps, organic photovoltaic devices exhibit unusual electrical and optical behavior. This affects the dark current voltage (*I*-*V*)characteristics and also the photocurrent. Traps are modeled by different workers in different ways such as discrete trap, multi traps, transport hopping via localized states, etc. But in all these cases, the trap energy is a very important parameter. Trap energy, which may be considered as the potential depth of the traps, has a major impact on the charge transport process of these devices. During transport, the free carriers interact with the traps and in the process a majority of these carriers get entrapped. Due to it, the motion of the carriers get slowed down. In other words, it may be considered that the traps behave as potential wells and the carriers reside and become immobilized within the traps. The residing time may be considered proportional to the depth or the energy of the traps for a particular concentration of the trap charge

---

Received May 27, 2015; accepted July 22, 2015

E-mail: nb_manik@yahoo.co.in

density. Due to this, the recombination and mobility of charge carriers get affected. With an increase in trap charge density, the recombination of charges increase and also the mobility gets reduced. For the last few years, we have been studying the effects of traps in organic dye based photovoltaic devices [12–17]. Efforts to reduce the trap energy of these devices are being carried out as it would lower the rate of recombination and thereby enhance the conduction of charges through these devices. Different approaches are being undertaken in this regard. By changing the device structure, incorporating different guest materials such as nanoparticles, carbon nanotubes (CNT), etc, researchers are trying to control the effect of traps and improve the performance of these organic dye based devices [18–20]. Reports suggest that CNTs help to enhance the efficiency of organic photovoltaic (OPV) devices [21,22]. In our previous work, we have observed that due to the addition of COOH- single walled carbon nanotubes (SWCNTs), the electrical and photovoltaic properties of Malachite Green dye based photovoltaic devices improved [23].

In the present work, we have investigated the changes in electrical and photovoltaic properties of methyl red (MR) dye based PEC in presence of SWCNT. Generally, in a PEC, an ionic salt is used in a solid matrix. In this work, we have used $LiClO_4$ as an ion source. poly (ethylene oxide) (PEO) of molecular weight 100000 is used as the solid polymeric matrix. $LiClO_4$ is mixed with solid polymer matrix PEO to form the solid-state ionic conductor. The ionic conductivity of PEO:$LiClO_4$ complexes is very low. To enhance the ionic conductivity EC and PC are used as plasticizers. Our earlier works [24] show that use of plasticizers ethylene carbonate (EC) and propylene carbonate (PC) assist charge migration. MR dye is used as the light sensitizer. We fabricated cells with this blend by drop casting on a spin coater. For fabrication of these cells, we used indium tin oxide (ITO) coated glass as the front electrode and aluminum (Al) coated on mylar (M) sheet as the back electrode. Next, we added SWCNT to this blend and fabricated cells in a similar manner. Our interest is to observe the change in electrical and photovoltaic properties of the MR cells due to addition of SWCNT. Such a study is important to understand the role of CNT in dye based PEC. After fabrication is done, all the cells are kept in vacuum for around 12 h before characterization.

2 Experiments

2.1 Materials

The structures of MR dye (Finar Chemicals, Ahmedabad, India, 99.5% pure) and SWCNT (Sisco Research Laboratories, India) are shown in Figs. 1(a) and 1(b), respectively. polyvinyl alcohol (PVA) has been purchased from S.D. Fine Chem. Ltd., Boisar, India and PEO from BDH, England, UK. We have procured $LiClO_4$, EC, PC from Fluka (99.5% pure). We have used ITO coated glass as the front electrode and Al coated with M sheet as the back electrode. It can be seen from our works [26] that Al-M has better optical reflectivity that Al. As a result of this back reflection, more optical energy can be confined in the organic dye.

As mentioned, we have chosen MR for our study as it is one of the less reported dyes in photovoltaic mode and has a good optical response. It is a typical aromatic azo dye with the chemical formula NC_6H_4COOH (2-[4-(dimethylamino) phenylazo] benzoic acid). The reddish color of MR comes from its absorbance in the visible region of the spectrum due to the delocalization of electron in the benzene and azo groups forming a conjugated system [27,28].

2.2 Sample preparation

For sample preparation, 1mg of PVA is added in 30 mL of double distilled water and stirred well to form a transparent viscous solution of PVA. Here, PVA acts as an inert binder. In this solution, 1 mg of MR dye is added and stirred well in a magnetic stirrer. In a separate beaker, a gel like electrolyte is prepared by mixing $LiClO_4$, PEO, EC and PC in the percentage weight ratio of 30.60%–3.60%–19.60%–46.20% by weight. This electrolyte is heated at around 60° C and stirred well in a magnetic stirrer for about 6 h. Then, this electrolyte is mixed with the previously prepared dye solution to form the ionic blend. This ionic blend is then spin coated on a ITO coated glass and Al-M electrodes and sandwiched to form the device. This blend is then separated into two parts in two beakers and in one of them we add SWCNT in the ratio 1:1 of MR dye and SWCNT and again stirred well.

Next we have fabricated different cells with these two

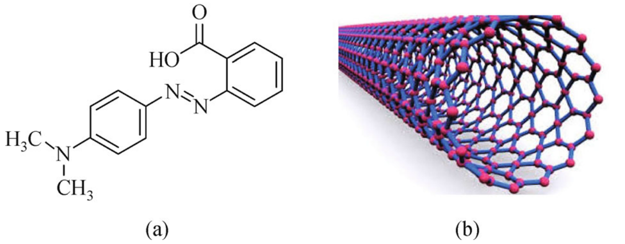

Fig. 1 Structure of (a) methyl red (MR) dye; (b) single walled carbon nanotubes [25]

blends. To prepare the cells, the MR dye blend is spin coated on a pre cleaned ITO coated glass at a speed of 2500 r/min and the film is semi-dried in vacuum. The same blend is drop cast on the Al-M electrode, which was placed on the spin coater. When both the electrodes are in semi-dry state, they are sandwiched together to form the MR dye based photoelectrochemical cell. By using the same procedure cell are prepared with the SWCNT mixed MR dye blend. All the cells have an area of 1.5 cm × 1.5 cm. The cells are kept in vacuum for 12 h before characterization. To make the system cost effective, we have used all the components including the MR dye and the electrodes in commercial grade and also the measurements were carried out in the open atmosphere of the laboratory. So, due to the less costly chemicals, the overall efficiency of the device is quite poor. Figure 2 shows the diagram of a typical photoelectrochemical cell.

3 Measurements

The absorption spectra of the cells are measured by using an Elico scanning mini spectrometer. Dark current voltage (*I*-*V*) characteristics of the cells have been measured with a Keithley 2400 source measure unit. During measurement, the bias voltage is varied from 0 to 6 V in steps of 0.5 V with 1500 ms delay. A solar simulator (Model 150 W Newport Corporation) has been used as the light source for the photovoltaic measurement. The photocurrent and photo voltage are measured with a digital current nanometer and Keithley 2000 multimeter, respectively. The light intensity is measured by a calibrated lux meter (Kyoritsu Electrical Instruments Works Ltd., Toyko, model 5200). Pulsed photocurrent measurements are done with an Agilent data-logger (Model 34970A) data acquisition system. The experiments have been done in the clean open atmosphere of the laboratory at a room temperature of 22°C.

4 Results and discussion

The absorption spectra of MR dye in doubled distilled water is shown in Fig. 3. As observed, MR shows a peak at 524 nm in distilled water. For comparison, the spectrum of SWCNT mixed with MR has also been shown. It is observed that due to addition of SWCNT there occur no significant changes in peak absorption wavelength of MR dye. From this observation, it can be interpreted that SWCNT has no significant role in the generation of charges carriers.

The dark *I*-*V* characteristics of the cells are shown in Figs. 4(a) and 4(b). From the curves, it is observed that after a certain transition voltage (V_{th}) the conduction mechanism of the cells change drastically. It is expected that at sufficiently low voltages the current increases in accordance with Ohm's law. As the applied voltage is increased, the injection of charges increase and the density of free carriers increase slowly. With the increase of free carriers, the charge trapping mechanism also increase and part of the free carriers become trapped. After a certain transition voltage, the density of trapped charges become higher and the current becomes trap limited. This process continues until another transition voltage is reached where the traps get filled up and the current becomes trap filled current. Here, in Figs. 4(a) and 4(b), it can be seen that even below the transition voltage, there is a certain considerable amount of current in both the cells. Also for the MR cell with SWCNT, the transition voltage shifts to a lower value from 2.52 to 1.99 V. But still a clear picture of the curves cannot be understood from the *I*-*V* curves and so we plotted the data on a logarithmic scale.

Figures 5 (a) and 5(b) show the dark *I*-*V* characteristics of the cells on a logarithmic scale. The curves show that there are three distinct regions of current conduction for both the cells. In these three regions, the mechanism of current conduction is different as mentioned above. In case of the MR cell without SWCNT, the first transition voltage (V_{th1}) is found to be at 2.52 V. Below this, the conduction mechanism is Ohmic. Above this voltage, the current is basically space charge limited in presence of exponentially distributed trap states. This mechanism continues until another transition voltage (V_{th2}) is reached when all the traps become filled up. After V_{th2}, again the current conduction mechanism changes and the current becomes trap filled current. For the MR cell without SWCNT, this

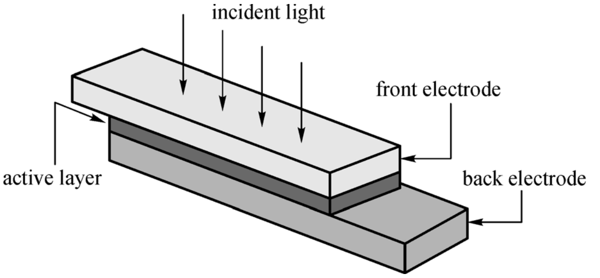

Fig. 2 Schematic diagram of the photoelectrochemical cell. Indium tin oxide (ITO) coated glass is used as the front electrode and a thin layer of aluminum (Al) coated on a mylar (M) sheet is used as the back electrode. Here, methyl red (MR) dye is used as a light sensitizer in the ionic blend comprising of $LiClO_4$, PEO, EC and PC

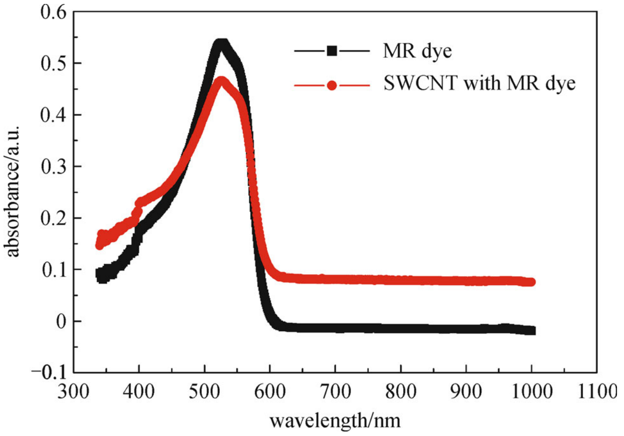

Fig. 3 Absorption spectra of methyl red (MR) and single walled carbon nanotube (SWCNT) mixed with MR in distilled water

second transition voltage is found to be at 4.2 V. The three regions mentioned above have been identified as region I, II and III in Figs. 5(a) and 5(b). In case of the MR cells with SWCNT, V_{th1} occurs at 1.99 V and V_{th2} at 3.55 V. Thereafter to estimate the slope of the curves and to estimate the trap energy, we recollect the *I*-*V* relation.

We already know that organic materials are disordered solids with no well-defined band structure. The molecules are bound together by weak van-der-Walls forces and the charge transport occurs through the loosely bound π-conjugated electrons. Here, instead of conduction and valence band, there are lowest unoccupied molecular orbital (LUMO) and highest occupied molecular orbital (HOMO) levels. These weak molecular bonds and structural disorders give rise to electronic traps in these systems, which are assumed to play a dominant role in the current conduction process.

According to Yang and Shen [29], these traps introduce energy levels inside the energy gap between the HOMO and LUMO levels of the organic layers. The entrapping and de-trapping of charges in these trap levels has a significant effect on the operation and performance of these

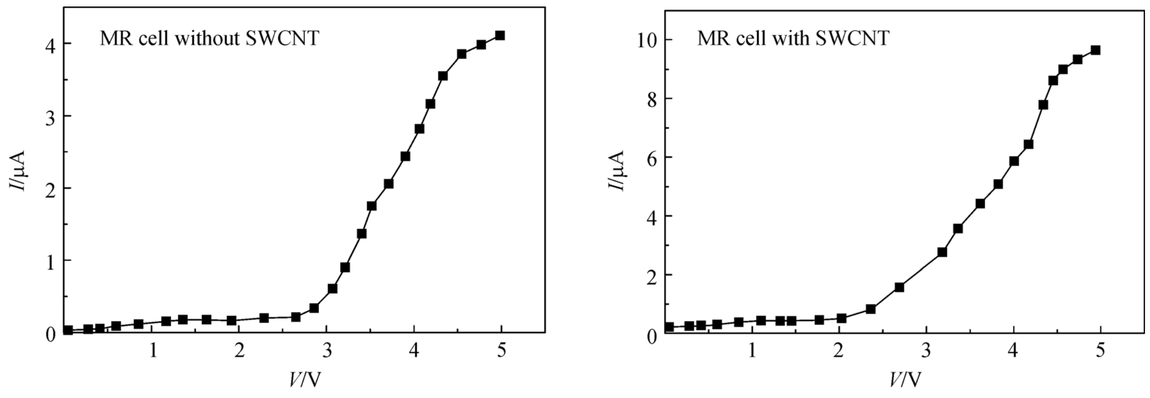

(a) (b)

Fig. 4 Dark *I*-*V* characteristics for (a) methyl red (MR) dye based cell and (b) single walled carbon nanotube (SWCNT) mixed with MR dye cell

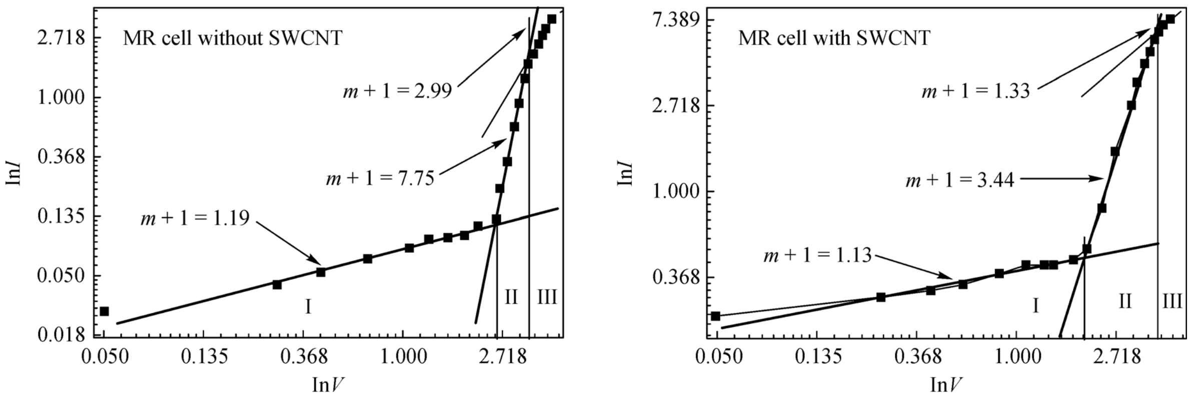

(a) (b)

Fig. 5 ln*I*-ln*V* characteristics for (a) methyl red (MR) dye based cell and (b) single walled carbon nanotube (SWCNT) mixed with MR dye cell photoelectrochemical cells. Because of the presence of traps in these devices, a large part of the injected charges get immobilized and result in crowding of charges near the electrodes. This kind of conduction process is usually referred to as the trap limited conduction process. This is a special case of the general space charge limited (SCL) regime [30]. The process is referred to as trap-free SCL conduction when the space charges are dominantly free carriers. The distribution of trap energy level is generally described by one of the following ways: 1) an exponential distribution, 2) discrete levels, and 3) a Gaussian distribution. Assuming an exponential energy distribution, trap charge concentration (n_t) may be expressed as

$$n_{\mathrm{t}} = H_n \exp\left(\frac{F_n}{kT_{\mathrm{c}}}\right), \tag{1}$$

where H_n is the trap density, F_n is the electron Fermi energy, K is Boltzmann constant, and T_c is characteristic temperature of the exponential trap distribution (i.e., $T_c = E_c/\mathrm{K}$, where E_c is the characteristic trap energy). Solving the Poisson equation with this form of trap distribution [31], the *I-V* characteristic is calculated and written in the following form:

$$J = N_{\mathrm{c}}\mu q^{1-m}\left[\frac{m\varepsilon}{H_n(m+1)}\right]^m\left(\frac{2m+1}{m+1}\right)^{m+1}\frac{V^{m+1}}{L^{2m+1}}, \tag{2}$$

where N_c is the effective density of states in LUMO or HOMO, μ is the mobility of majority carrier, L is the thickness of the layer, ε is equal to $\varepsilon_0\varepsilon_r$ with ε_0 being the permittivity of vacuum and ε_r the dielectric constant, V is the applied voltage and $m = T_c/T$, T_c is a characteristic temperature that describe the trap distribution. The most notable feature in the above equation is the power law dependence of

$$J \sim V^{m+1}. \tag{3}$$

In this work, the dark *I-V* curves have been analyzed to find the characteristic temperature T_c and from it the characteristic trap energy E_c. Figures 5(a) and 5(b) show the logarithmic plots of the dark *I-V* curves. From these figure, we can calculate the '$m + 1$' values for the different cells using Eq. (3) and estimate the trap energy of the cells and analyze the change in the conduction behavior of the charges due to the addition of SWCNT. From those values, we have extracted the values of characteristic trap energy of the system. The values are shown in Table 1.

The trap energy is a very important parameter controlling the conduction of charges in these devices. Depending on the energy values of traps, the immobilization time of trapped carriers also varies. So any changes in trap energy will affect the overall performance of the devices. From the values calculated in Table 1, it is observed that both V_{th} and E_c have decreased in presence of SWCNT. Decrease in trap energy indicates that the residing time or the immobilized time of the charges will decrease. This leads to fast collection of charges. It is expected that this process will reduce recombination and will enhance the device performance. To ensure this, we will also perform the photovoltaic measurements.

Figures 6(a) and 6(b) show the photovoltaic characteristics of the cells. The curves are obtained by varying the load resistance. Different photovoltaic parameters such as open circuit voltage (V_{oc}), short circuit current density (J_{sc}), fill factor (*FF*) and power conversion efficiency (η) of the cells are evaluated from the curves and are listed in Table 2.

From the results obtained, it is seen that V_{oc}, J_{sc}, *FF* and η values have increased for the MR cell in presence of SWCNT. It is also observed that there is a significant change in the short circuit current density but the open circuit voltage of the cells does not change considerably. For the MR cells with SWCNT, the *FF* increased from 0.38 to 0.48. It can be expected that due to a decrease in trap energy, charge conduction process becomes faster and causes an increase in the output current and overall device performance.

To further ensure this fact that decrease in trap energy causes faster migration of charges, we performed the transient photocurrent measurements. The charge separation and relaxation dynamics of the cells can be understood from the pulsed photocurrent measurements. Figures 7(a) and 7(b) show the transient photo-response of the cells. We have performed the measurements with different light

Table 1 Extraction of values of 'm' and trap energy 'E_c' from ln*I*-ln*V* curves

cell type	V_{th1}/V	V_{th2}/V	m_1 region I	m_2 region II	m_3 region III	E_c in region II/eV
MR cell without SWCNT	2.52	4.2	1.19	4.61	1.99	0.091
MR cell with SWCNT	1.99	3.55	1.13	3.42	0.33	0.061

Table 2 Different photovoltaic parameters extracted from the light *I-V* curves

cell type	cell area/cm^2	J_{sc}/(μA·cm^{-2})	V_{oc}/mV	*FF*	η/10^{-2}%
MR cell without SWCNT	1.5	296.92	79.35	0.38	1.12
MR cell with SWCNT	1.5	734.26	195	0.48	68.7

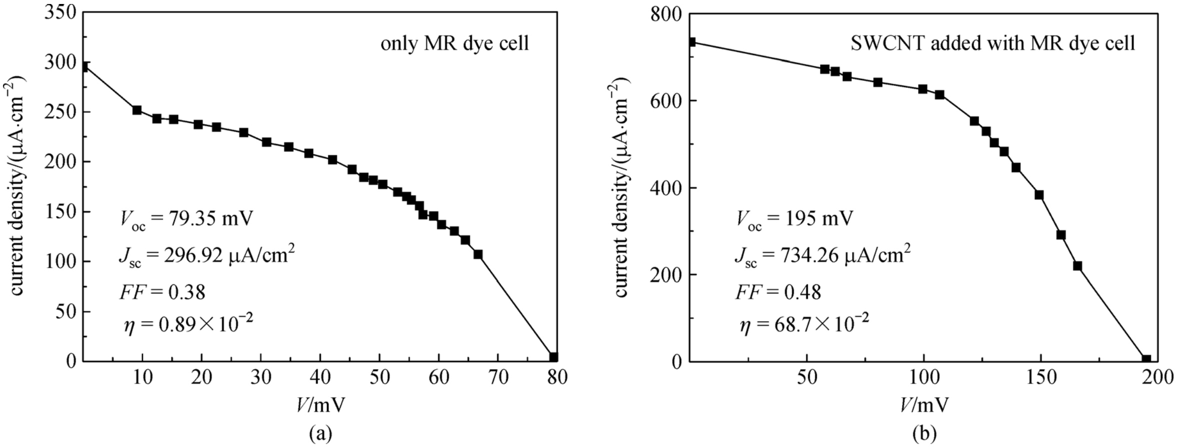

Photovoltaic characteristics of (a) methyl red (MR) cell and (b) single walled carbon nanotube (SWCNT) mixed with MR cell. Different photovoltaic parameters such V_{oc}, J_{sc}, FF and η have been extracted from the curves, the values of which are shown in Table 2

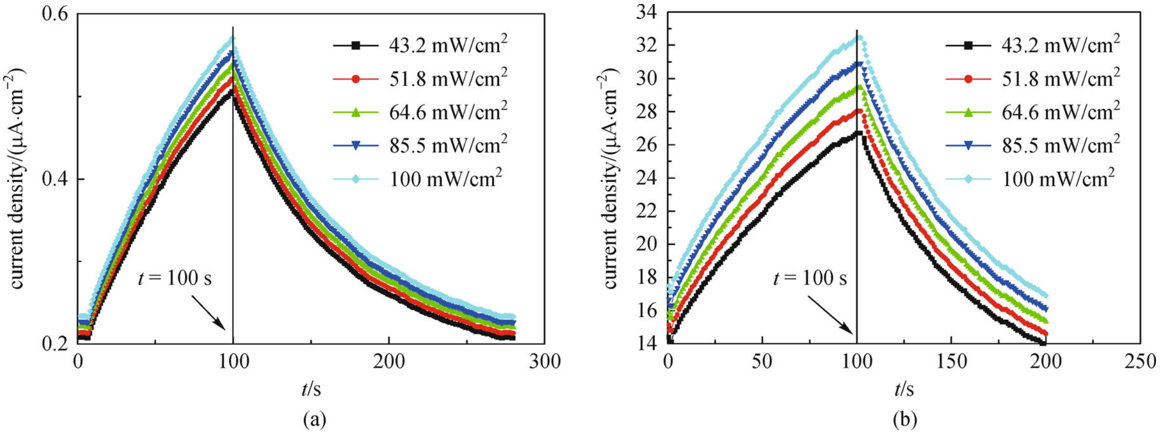

Fig. 7 Pulsed photocurrent measurements for (a) only (a) methyl red (MR) cell and (b) single walled carbon nanotube (SWCNT) mixed with MR cell

intensity. To perform the measurement, the cell is exposed to radiation for about 100 s and then radiation is turned off. The growth and decay rate for the two cells are observed to be quite different. From the curves shown in Fig. 8, it is observed that the photocurrent growth and decay rate for SWCNT added MR cells are quite faster. A sharp increase and decrease in photocurrent indicates that the charge separation rate is fast and charge recombination is reduced. Analysis of this data will give further information about the charge transport mechanism of the system.

To investigate more critically, we consider the curves for particular incident intensity. Figures 8(a) and 8(b) shows the pulsed photocurrent measurements of the cells for an incident radiation of 100 mW/cm^2. From the curves, it can be seen that the growth and decay rate of photocurrent for the two cells are quite different. For the MR cell without SWCNT, the photocurrent decays for a long time and takes around 175 s to attain the initial value. While in presence of SWCNT, the decay is quite faster, and the photocurrent takes around 100 s to decay. Also the peak value of photocurrent is higher in presence of SWCNT.

To study further this decay process, we fitted the decay current with time in a logarithmic scale, as shown in Figs. 9 (a) and 9(b). It is interesting to note that for both the cells the decay current is fitted and found to follow a power law relation with time, which can be expressed as $I_{ph} \sim t^{\alpha}$, where I_{ph} is the photocurrent and α is the decay constant. Here, the value of this decay constant is found to be 0.96 and 0.055 for the MR cells with and without SWCNT, respectively.

From this power law relation of photocurrent with time, we also get some idea about the charge transport mechanism. Power law relation indicates a dispersive transport via hopping in between localized trap states. This may be presented in a schematic diagram. Figures 10(a) and 10(b) show the charging and discharging process of

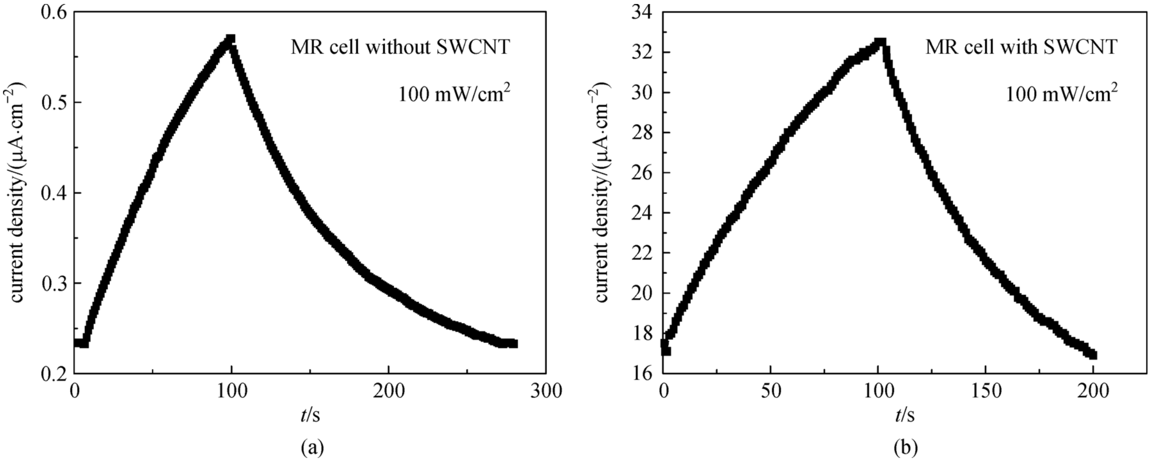

Fig. 8 Pulsed photocurrent measurements of (a) (a) methyl red (MR) cell and (b) single walled carbon nanotube (SWCNT) mixed with MR for an incident radiation of 100 mW/cm^2

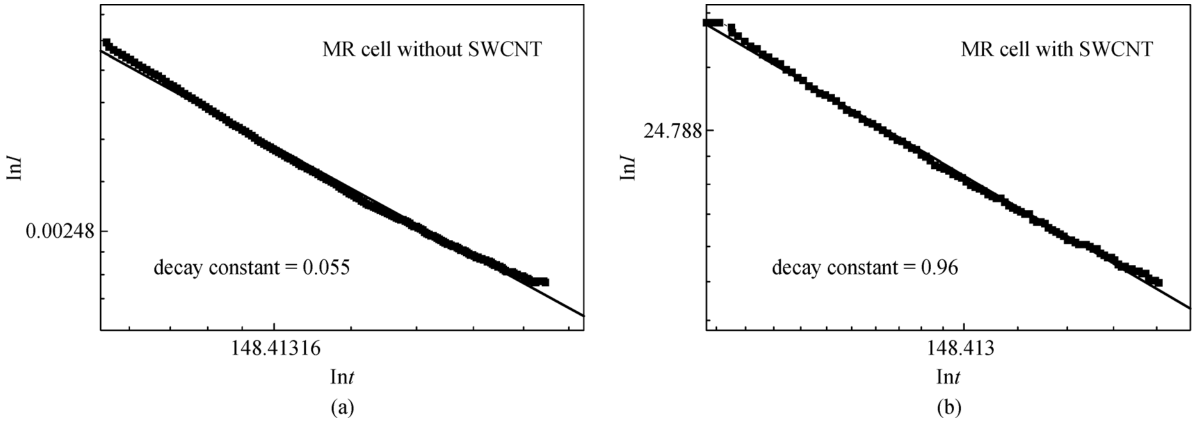

Fig. 9 Determination of decay constant from ln*I*-ln*t* curves for (a) methyl red (MR) cell without single walled carbon nanotube (SWCNT) and (b) MR cell with SWCNT

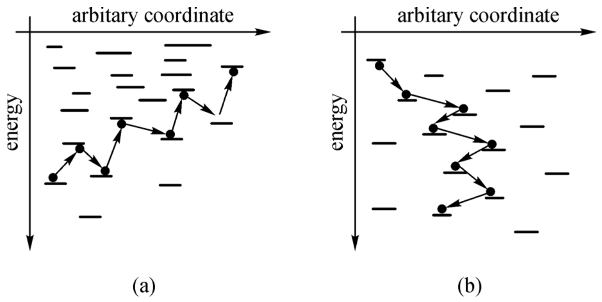

Fig. 10 (a) Charging and (b) discharging of trapped carriers during photocurrent growth and decay

the charge carriers in between the traps during the growth and decay of the photocurrent respectively. During growth of photocurrent, the traps get charged and the trapped charges go to the higher energy levels. While during decay the carriers hop from higher energy states to lower energy states. In this process, majority of the carriers get released from the traps while a number of carriers are lost due to recombination.

It is expected that addition of SWCNT lowers the trap energy by providing efficient percolation pathways for conduction of charges. To get an overall view of the different parameters affected due to addition of SWCNT, the comparison has been shown in Table 3. From this table, we get a clear idea that the electrical and photovoltaic properties of the MR cells change in presence of SWCNT.

5 Conclusions

In this work, we report on the changes in electrical and photovoltaic properties of MR dye based photoelectrochemical cells in presence of SWCNT. Dark *I*-*V* analysis shows that three different types of current conduction mechanisms occur with the applied bias voltage. Our

Table 3 Comparison of the different parameters extracted from the electrical and optical measurement of the MR cells with and without SWCNT

Parameter	without SWCNT	with SWCNT
trap energy (E_c)	0.172 eV	0.062 eV
transition voltage (V_{th1})	2.52 V	1.99 V
transition voltage (V_{th2})	3.55 V	4.2 V
short circuit current (J_{sc})	296.92 μA/cm^2	734.26 μA/cm^2
open circuit voltage (V_{oc})	79.35 mV	195 mV
fill factor (*FF*)	0.38	0.48
decay constant	0.055	0.096

results show that due to addition of SWCNT the trap energy of the cells decrease from 0.172 to 0.062 eV. Consequently for the same devices, there is about 79% increase in *FF*. The V_{oc}, J_{sc} and *FF* are 195 mV, 734.26 μA/cm^2 and 0.48 respectively for the SWCNT added MR cell. To investigate further the role of SWCNT, transient photocurrent measurement performed and the photocurrent growth and decay rate is found to be faster in presence of SWCNT. By fitting the data of a logarithmic scale, it is found that the photocurrent follow a power law relation with time. From this, the decay constant is estimated and found to be 0.96 and 0.055 for the MR cells with and without SWCNT respectively. It is expected that SWCNT provide effective percolation pathways for conduction of charges. Due to presence of SWCNT, the trap energy of the cells get reduced. Due to decrease in trap energy, the residing time of the charge carriers in the traps also decrease since it is expected that the residing time of the trapped carriers is proportional to the depth or the energy value of the traps. This leads to better current conduction and improves the photovoltaic action of the cells. Further work is going on to understand the role of carbon nanotubes on the charge recombination process of organic dye based photoelectrochemical cells.

Acknowledgements The authors thank University Grant Commission (UGC), India and Council of Scientific and Industrial Research (CSIR), India for providing financial support for carrying out the research work.

References

1. Grätzel M. Photoelectrochemical cells. Nature, 2001, 414(6861): 338–344
2. Hagberg D P, Marinado T, Karlsson K M, Nonomura K, Qin P, Boschloo G, Brinck T, Hagfeldt A, Sun L. Tuning the HOMO and LUMO energy levels of organic chromophores for dye sensitized solar cells. Journal of Organic Chemistry, 2007, 72(25): 9550–9556
3. Haldar A, Maity S, Manik N B. Electrical and photovoltaic characterisations of methyl red dye doped solid-state photoelectrochemical cell. Ionics, 2009, 15(1): 79–83
4. Burke D J, Lipomi D J. Green chemistry for organic solar cells. Energy & Environmental Science, 2013, 6(7): 2053–2066
5. Hardin B E, Snaith H J, McGehee M D. The renaissance of dye-sensitized solar cells. Nature Photonics, 2012, 6(3): 162–169
6. Li G, Zhu R, Yang Y. Polymer solar cells. Nature Photonics, 2012, 6 (3): 153–161
7. Islam M R, Maity S, Haldar A, Manik N B, Basu A N. Photocurrent growth and decay behaviour of crystal violet dye-based photoelectrochemical cell in photovoltaic mode. Ionics, 2012, 18(1–2): 209–214
8. Singh P K, Jadhav N A, Mishra S K, Singh U P, Bhattacharya B. Application of ionic liquid doped solid polymer electrolyte. Ionics, 2010, 16(7): 645–648
9. Fredin K, Nissfolk J, Boschloo G, Hagfeldt A. The influence of cations on charge accumulation in dye sensitized solar cells. Journal of Electroanalytical Chemistry, 2007, 609(2): 55–60
10. Shuttle C G, Treat N D, Douglas J D, Fréchet J M J, Chabinyc M L. Deep energetic trap states in organic photovoltaic devices. Advanced Energy Materials, 2012, 2(1): 111–119
11. Walker A B, Peter L M, Martínez D, Lobato K. Transient photocurrents in dye-sensitized nanocrystalline solar cells. CHIMIA International Journal for Chemistry, 2007, 61(12): 792–795
12. Li C, Duan L, Li H, Qiu Y. Universal trap effect in carrier transport of disordered organic semiconductors: transition from shallow trapping to deep trapping. Journal of Physical Chemistry C, 2014, 118(20): 10651–10660
13. Montero J M, Bisquert J. Trap origin of field-dependent mobility of the carrier transport in organic layers. Solid-State Electronics, 2011, 55(1): 1–4
14. Carr J A, Chaudhary S. On the identification of deeper defect levels in organic photovoltaic devices. Journal of Applied Physics, 2013, 114(6): 064509
15. Mandoc M M, Kooistra F B, Hummelen J C, de Boer B, Blom P W M. Effect of traps on the performance of bulk heterojunction organic solar cells. Applied Physics Letters, 2007, 91(26): 263505
16. Dey S K, Islam M R, Manik N B, Basu A N. Study on the effect of trap levels on steady-state dark $I-V$ characteristics in Safranine-T-based solid-state thin film photoelectrochemical cell. Journal of Materials Science Materials in Electronics, 2002, 13(5): 249–252
17. Islam M R, Saha S, Manik N B, Basu A N. Transient current study in Safranine-T dye based organic photo-electrochemical cell using exponentially distributed trap assisted charge transport model. Indian Journal of Physics, 2012, 86(12): 1101–1106
18. Chen J, Yan Y, Lin K. Effects of carbon nanotubes on dye-sensitized solar cells. Journal of the Chilean Chemical Society, 2010, 57(5B):

1180–1184

19. Hosni M, Kusumawati Y, Farhat S, Jouini N, Pauporté T. Effects of oxide nanoparticle size and shape on electronic structure, charge transport and recombination in dye-sensitized solar cell photoelectrodes. Journal of Physical Chemistry C, 2014, 118 (30): 16791–16798
20. Ausman K D, Piner R, Lourie O, Ruoff R S. Organic solvent dispersions of single-walled carbon nanotubes: towards solutions of pristine nanotubes. Journal of Physical Chemistry B, 2000, 104 (38): 8911–8915
21. Lee K M, Hu C W, Chen H W, Ho K C. Incorporating carbon nanotube in a low-temperature fabrication process for dye-sensitized TiO_2 solar cells. Solar Energy Materials and Solar Cells, 2008, 92 (12): 1628–1633
22. Somani S P, Somani P R, Umeno M. Carbon nanotube incorporation: a new route to improve the performance of organic-inorganic heterojunction solar cells. Diamond and Related Materials, 2008, 17 (4–5): 585–588
23. Chakraborty S, Manik N B. Effect of COOH-functionalized SWCNT addition on the electrical and photovoltaic characteristics of Malachite Green dye based photovoltaic cells. Journal of Semiconductors, 2014, 35 (12): 124004
24. Maity S, Haldar A, Manik N B. Effect of plasticizer on Safranine-T-dye-based solid-state photo electrochemical cell. Ionics, 2008, 14 (6): 549–554
25. Alam A, Sachar S, Puri N, Saxena R K. Interactions of polydispersed single-walled carbon nanotubes with T cells resulting in downregulation of allogeneic CTL responses in vitro and in vivo. Nanotoxicology, 2013, 7(8): 1351–1360
26. Haldar A, Maity S, Manik N B. Effect of back electrode on photovoltaic properties of crystal-violet-dye-doped solid-state thin film. Ionics, 2008, 14(5): 427–432
27. Mahmoud M A, Poncheri A, Badr Y, Abd El Wahed M G. Photocatalytic degradation of methyl red dye: research letter. South African Journal of Science, 2009, 105(7–8): 299–303
28. Buitrón G, Quezada M, Moreno G. Aerobic degradation of the azo dye acid red 151 in a sequencing batch biofilter. Bioresource Technology, 2004, 92(2): 143–149
29. Yang J, Shen J. Effects of discrete trap levels on organic light emitting diodes. Journal of Applied Physics, 1999, 85(5): 2699–2705
30. Shen J, Yang J. Physical mechanisms in double-carrier trap-charge limited transport processes in organic electroluminescent devices: A numerical study. Journal of Applied Physics, 1998, 83(12): 7706–7714
31. Mark P, Helfrich W. Space-charge-limited currents in organic crystals. Journal of Applied Physics, 1962, 33(1): 205–215

Sujata Chakraborty received her B.Sc. degree from the Department of Physics at Cotton College under Gauhati University, India in 2009 and obtained her M.Sc. degree from the same university in 2011. She is now a Ph.D. student at the Department of Physics, Jadavpur University. Her research interests include development and characterization of photovoltaic devices using semiconducting conjugated polymers and organic dyes.

Nabin Baran Manik is an associate professor in Department of Physics, Jadavpur University, Kolkata, India. He received his Ph.D. degree from Jadavpur University, Kolkata, India, in 1998 and right after that he joined as lecturer in Physics Department of the same university. In 2004, he was awarded Better Opportunities for Young Scientists in Chosen Areas of Science and Technology (BOYSCAST) Fellowship of Department of Science and Technology (DST), Govt. of India and did his Post Doctoral work at Leibniz-Institut für Festkörper- und Werkstoffforschung (IFW), Dresden, Germany. He is working in the area of development of photovoltaic devices using semiconducting conjugated polymers and organic dyes, low temperature instrumentation, characterization of optoelectronics devices at low temperature. Several students have completed their Ph.D. under his supervision. Different research projects from different funding agencies were undertaken by him. He had also delivered invited talk in different national and international conference. He has different publications both at national and international journals some of which are available in his website: www.nbmanik.in.